Excited State Processes of Dinuclear Pt(II) Complexes Bridged by 8-hydroxyquinoline

ARTICLE

Excited State Processes of Dinuclear Pt(II) Complexes Bridged by 8-hydroxyquinoline

Sarah Kromer,[a, †] Subhangi Roy,[a, †] James E. Yarnell,[a] Chelsea M. Taliaferro[a] and Felix N. Castellano*[a]

Dinuclear d^8 Pt(II) complexes, where two mononuclear square planar Pt(II) units are bridged in an "A-frame" geometry, possess photophysical properties characterised by either metal-to-ligand- (MLCT) or metal-metal-ligand-to-ligand charge transfer (MMLCT) transitions determined by the distance between the two Pt(II) centres. When using 8-hydroxyquinoline (8HQH) as the bridging ligand to construct novel dinuclear complexes with general formula [C^NPt(μ-8HQ)]$_2$, where C^N is either 2-phenylpyridine (**1**) or 7,8-benzoquinoline (**2**), triplet ligand-centered (^{3}LC) photophysics results echoing that in a mononuclear model chromophore, [Pt(8HQ)$_2$] (**3**). The lengthened Pt-Pt distances of 3.255 Å (**1**) and 3.243 Å (**2**) results in a lowest energy absorption centred around 480 nm assigned as having mixed MLCT/LC character by TD-DFT, mirroring the visible absorption spectrum of **3**. Additionally, **1** and **2** exhibit ^{3}LC photoluminescence with limited quantum yields (0.008) from broad transitions centred near 680 nm. Photoexcitation of **1-3** leads to an initially prepared excited state that relaxes within 15 ps to a ^{3}LC excited state centred on the 8HQ bridge, which then persists for several microseconds. All the experimental results correspond well with DFT electronic structure calculations.

Introduction

Square planar Pt(II) complexes have sparked increased research interest in recent years due to their unique photophysical properties originating from strong spin-orbit coupling and the resulting range of available excited states.[1-4] For instance, long-lived excited states with high photoluminescence (PL) quantum yields often observed from Pt(II) complexes find applications in different areas of modern photochemistry and photophysics.[1,5-7] Additionally, structural deformation and intermolecular interaction of Pt(II) complexes can change spectroscopic properties and provide a tool for tuning photoluminescence properties.[8-14] Among different Pt(II) species, square-planar cyclometalated complexes are an important class of compounds illustrated by a number applications in such areas as optoelectronic devices, temperature, pH, and cation sensing, volatile organic vapour detection, as well as in photocatalysis.[5-7,15-26] Interest in these complexes is motivated in part by the cyclometalation effect which improves their stability and PL efficiency.[27-31] One important consequence on the photophysical properties is that the energy of the deactivating metal-centred d−d excited states are raised substantially relative to those of complexes bearing only neutral diimine ligands. Accordingly, cyclometalation offers an effective tool for preparing efficient photoluminescent compounds based on Pt(II).

Of particular interest are dinuclear Pt(II) complexes bridged by various heterocyclic ligands due to their role in furthering understanding of metal-metal interactions in excited states, as well as their applicability towards new light harvesting molecular materials.[32] Cyclometalated Pt(II) dinuclear complexes provide unique opportunities to tune photophysical properties through fine adjustments in relevant ligand structures. Manipulation of the Pt-Pt distance by incorporating bulky substituents into the bridging ligands produces complexes whose excited state character is dominated by metal center orbital overlap, revealing metal-metal-to-ligand charge-transfer (MMLCT) transitions. Dinuclear complexes lacking such metal-metal interactions instead exhibit ligand-centered (LC) or metal-to-ligand charge transfer (MLCT) transitions, as is characteristic of mononuclear Pt(II) complexes.[32] The MMLCT transition promotes an electron from a filled Pt-Pt centered $5d_z^2$-$5d_z^2$ (σ^*) orbital, terminating on an empty cyclometalating ligand-centered (π^*) orbital. This leads to a photoinduced structural change as light excitation instantaneously increases the metal-metal bond order, inducing Pt-Pt bond contraction. The resulting transiently formed Pt-Pt σ-bond and its vibrational motion renders these dinuclear complexes model systems for deciphering coherence phenomena in molecular excited states.[33-44]

Among the various studies into Pt(II) complexes, pyrazolate bridging ligands have been extensively used in conjunction with bidentate C^N cyclometalating ligands.[45-52] Specifically, a series of pyrazolate-bridged platinum(II) complexes with the general formula [C^NPt(pz')$_2$PtC^N] (where C^N = 2-(2,4-difluorophenyl)pyridyl, pz' = μ-pyrazolate) was reported by the

a. Department of Chemistry, North Carolina State University, Raleigh, NC 27695-8204.
† Electronic Supplementary Information (ESI) available: Structural characterization data, transient absorption and PL data, and frontier molecular orbitals for **1**- **3**. See DOI: 10.1039/x0xx00000x
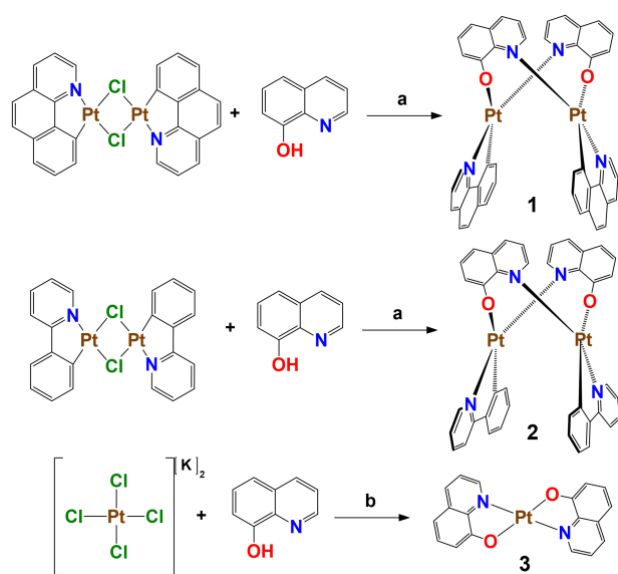
Scheme 1. Synthetic route for the preparation of **1** and **2**; a = K₂CO₃, 1,2-dicholoroethane, reflux, 24h.[53] Preparation of **3** where b = glacial acetic acid/H₂O, NaOH, reflux, 1h.[55]

Thompson group in 2005.[50] Through systematic variation of the size of the substituents pendant in the 3,5-positions of the pyrazolate bridge, it was shown that the bridging ligands control the degree of the metal-metal interaction and thus the observed excited state properties.

More recently, we have reported dinuclear Pt(II) complexes featuring substituted 2-hydroxypyridine and 2-thiolpyridine bridging ligands that exhibit MMLCT excited states.[53,54] It was observed that the 2-hydroxypyridine bridging ligands influenced ground and excited state properties of these dinuclear molecules by modulating the electronic structure of frontier orbitals through controlling the intramolecular metal-metal interaction. In this series of molecules, X-ray crystallography revealed Pt–Pt distances ranging between 2.815 and 2.878 Å; the former represents the shortest reported metal–metal distance for platinum(II) dinuclear species possessing low-energy MMLCT transitions. Use of a similar ligand, 8-hydroxyquinoline (8HQH), in Pt(II) mononuclear complexes is previously reported to have resulted in long-lived excited states.[55] Although the low lying LC excited states of coordinated 8-oxo-quinoline (8HQ) can be utilized for mixing with MLCT/MMLCT character, it had yet to be used as a bridging ligand in newly conceived Pt(II) dinuclear molecules.

In the present study, the dinuclear Pt(II) complexes [Pt(bzq)(μ-8HQ)]₂ (**1**) and [Pt(ppy)(μ-8HQ)]₂ (**2**) (bzq = 7,8-benzoquinoline and ppy = 2-phenylpyridine) were synthesized. Additionally, a previously reported mononuclear model complex, [Pt(8HQ)₂] (**3**) was also synthesized for comparison of observed spectroscopic properties. The dinuclear complexes were synthesized by ligand substitution reactions in high yields and characterized using multiple analytical techniques including ¹H NMR, elemental analysis, and high-resolution mass spectrometry (HRMS). The static and dynamic spectroscopic

properties of **1** and **2** were investigated using absorption, photoluminescence, and transient absorption spectroscopy, and subsequently compared with previously reported complexes of similar structure as well as **3**. In this analysis, it was found that [Pt(bzq)(μ-8HQ)]₂ and [Pt(ppy)(μ-8HQ)]₂ do not produce MMLCT excited states, but rather upon photoexcitation these complexes quickly form long-lived (μs) ^{3}LC excited states localized on the 8HQ bridge. The experimental observations correspond well with DFT calculations which implies that the triplet density of the lowest lying excited state lies primarily on the 8HQ bridging ligand.

Experimental

Reagents and Chemicals

An inert dry N₂ atmosphere was maintained during all synthetic manipulations using both normal and Schlenk glassware. All reagents and solvents were purchased from VWR or Sigma-Aldrich and used as received. The precursors, [Pt(DMSO)₂Cl₂] and the intermediate cyclometalated dichloro-bridged platinum(II) dinuclear complexes, [Pt(bzq)(μ-Cl)]₂ and [Pt(ppy)(μ-Cl)]₂, were synthesized according to their published procedures.[46,53,56,57] Spectroscopic samples were prepared air-free in a glovebox using spectroscopic-grade tetrahydrofuran (THF).

Synthesis

Both **1** and **2** were synthesized by slight modification of the previously published procedure.[53] A general synthetic route is given in Scheme 1. In short, [Pt(ppy)(μ-Cl)]₂ (621 mg, 0.807 mmol, 1 equiv. and 8HQH (307 mg, 2.11 mmol, 2.6 equiv.) were dissolved in 1,2-dichloroethane (80 mL) in a round bottom flask and in the presence of excess K₂CO₃. The reaction mixture was refluxed under N₂ for 24 hrs. Excess unreacted K₂CO₃ was subsequently filtered, and the resulting solution was evaporated under reduced pressure. The crude solid product was washed with acetonitrile, sonicated, and then filtered. The dark red solid was collected on a fritted funnel (635 mg, yield = 78.6%). The synthesis of **3** utilized the literature method.[55]

*anti-***[Pt(bzq)(μ-8HQ)]₂ (1)**: ¹H NMR (400 MHz, CD₂Cl₂) δ 9.55 (dd, J = 5.3, 1.2 Hz, 2H), 9.44 (dd, J = 5.2, 1.2 Hz, 2H), 8.38 (m, 4H), 7.87 (dd, J = 6.8, 1.6 Hz, 2H), 7.83 (d, J = 8.8 Hz, 2H), 7.67 (m, 4H), 7.63 (d, J= 8.8 Hz, 2H), 7.59 (dd, J = 8 Hz, 5.6Hz, 2H), 7.55-7.49 (m, 4H), 7.10 (dd, J = 7.8, 1.0 Hz, 2H), 6.98 (dd, J = 7.9, 0.9 Hz, 2H). HRMS, ESI: m/z 1035.1571, calculated [M+H] = 1035.1586. Elemental Analysis (%) calcd for C₄₄H₂₈N₄O₂Pt₂·2H₂O: C, 49.35; H, 3.01; N, 5.23. Found: C, 49.32; H, 3.27; N, 4.97%. Calc.

*anti-***[Pt(ppy)(8HQ)]₂ (2)**: ¹H NMR (400 MHz, CD₂Cl₂) δ 9.41 (d, J = 5.8 Hz, 2H), 9.26 (dd, J = 5.2, 0.8 Hz, 2H), 8.38 (dd, J = 8.4, 1.2 Hz, 2H), 7.90 (ddd, J = 8.2, 8.0, 1.2 Hz, 2H), 7.74 (d, J = 8 Hz, 2H), 7.63 (d, J = 7.6 Hz, 2H), 7.59 (dd, J = 7.6, 1 Hz, 2H), 7.53 − 7.46 (m, 4H), 7.32- 7.22 (m, 4H), 7.18 (ddd, J = 7.5, 7.2, 1.1 Hz, 2H), 7.04 (dd, J = 8, 1 Hz, 2H), 6.96 (d, J = 8, 1 Hz, 2H). HRMS, ESI: m/z

987.1574, calculated [M+H] = 987.1586. Elemental Analysis (%) calcd for $C_{40}H_{28}N_4O_2Pt_2 \cdot 1.25H_2O$: C, 47.60; H, 3.05; N, 5.55. Found: C, 47.92; H, 3.33; N, 5.26.

General Techniques

All the ^1H NMR spectra were recorded on a Varian Innova 400 NMR spectrometer operating at 400 MHz. High-resolution electrospray ionization mass spectrometry (ESI-HRMS) was performed at the Michigan State University Mass Spectrometry Facility. Elemental analyses were determined by Atlantic Microlab, Inc., Norcross, GA. Electronic absorption spectra were measured on a Shimadzu UV-3600 spectrometer. An Edinburgh FS-920 spectrofluorometer instrument was used to obtain the steady-state photoluminescence spectra. PL quantum yield measurements were performed on degassed samples using [Ru(bpy)$_3$](PF$_6$)$_2$ in acetonitrile as a relative standard.

Nanosecond Transient Absorption Spectroscopy

Nanosecond transient absorption difference spectra were collected at room temperature with an LP920 laser flash photolysis system (Edinburgh Instruments) using the Vibrant 355 LD-UVM Nd:YAG/OPO system (OPOTEK) as the excitation source (λ_{ex} = 500 nm, ~2.2 mJ/pulse). Spectral absorption difference spectra were collected with an iStar ICCD camera (Andor Technology), which was controlled by the LP-920 software program (Edinburgh Instruments). Sample optical density was maintained at approximately 0.3 – 0.8 and each was prepared by either degassing with N$_2$ for 30 minutes or in an air-free N$_2$ glove-box environment. Kinetic decay fittings were done utilizing Origin 2021b.

Femtosecond Transient Absorption Spectroscopy

Femtosecond transient absorption spectroscopy was undergone using equipment from the Imaging and Kinetic Spectroscopy (IMAKS) Laboratory at NCSU. Specifically, a 1 kHz Ti:Sapphire Coherent Libra regenerative amplifier was utilized to generate the initial 800 nm beam which was subsequently split to form the pump and probe beams. The 500 nm pump beam for excitation was generated inside an OperA Solo parametric amplifier (Coherent) and focused inside an Ultrafast Systems Helios transient absorption spectrometer. The probe beam was formed by focusing the residual 800 nm output into a sapphire crystal to generate the white light continuum. Within the spectrometer the pump and probe beams were overlapped within a 2 mm pathlength cuvette. The sample was stirred throughout each measurement and was analysed by static UV-Vis spectroscopy before and after each measurement to ensure there was no sample decomposition.

Computational Details

Electronic structure calculations on **1**-**3** were performed using the Gaussian 09 software package (revision D.01)[58] and the computation resources of the North Carolina State University High Performance Computing Center. Ground state geometry
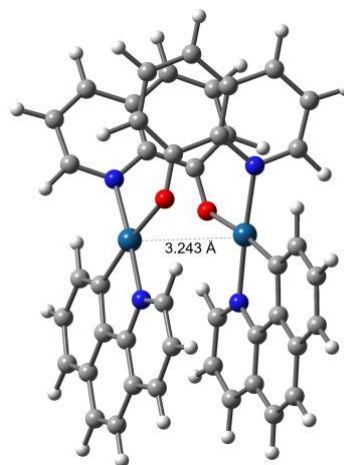

Fig. 1 DFT optimized structure of **1**, calculated at the PCM-PBE0-D3/Def2-SVP/SDD level of theory

optimization calculations were performed on the ground state and the lowest energy triplet state using density functional theory (DFT) and the PBE0-D3 functional.[59,63] The Def2-SVP basis set was utilized for all atoms with the effective core potential (ECP) being included for the platinum atoms.[60,61] The polarizable continuum model (PCM) was used to simulate the effects of the tetrahydrofuran solvent environment for all calculations.[62] Frequency calculations were performed on all ground state and triplet state structures and produced no imaginary frequencies. Time dependent density functional theory (TD-DFT) calculations were executed on the optimized ground-state geometries using the PBE0 functional mentioned previously. The energy and oscillator strength were computed for each of the 50 lowest singlet excitations and 10 lowest triplet excitations.

Results and Discussion

Synthesis and Structural Characterization

The synthesis of novel complexes **1** and **2** was achieved by following published procedures.[46,53] Both complexes were completely characterized by ^1H, ^{13}C NMR, high-resolution mass spectrometry and elemental analysis (see Electronic Supporting Information, ESI, Figs. S1-S6). Chromophore **3** was synthesized according to literature methods and is also presented in Scheme 1.[55]

DFT calculations

The optimized geometries and electronic structures of the Pt(II) complexes presented here were calculated at the PCM-PBE0-D3/Def2-SVP/SDD level of theory. This functional and basis set combination was successfully benchmarked in a prior study which compared the crystal structures of analogous complexes to their optimized geometries.[53] The functionals used included B3LYP, M06, and PBE0, and addition of the GD3 dispersion correction further improved the optimized structures with the PBE0-D3 performing the best out of the three.[53,64] In the present study, optimized ground state structures of **1** and **2**
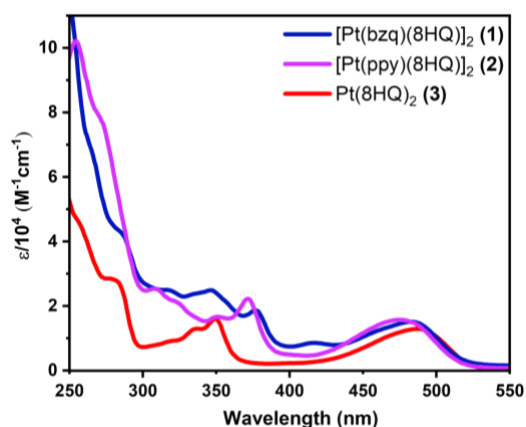
Fig. 2 Electronic absorption spectra of **1** – **3** measured in THF.

utilizing the PBEO-D3 functional were shown to have an A-frame geometry as observed in molecules of similar ligand structure. The complexes studied here, however, differ from analogous species in their Pt-Pt distances, 3.255 Å (**1**, Fig. 1) and 3.243 Å (**2**, Fig. S7), which are significantly longer than those bridged by hydroxypyridines (2.815-2.878 Å)[53] or thiolpyridine (2.849 Å).[64] Additionally, the triplet spin density was calculated for both **1** and **2** with much of the singly occupied orbitals residing on the 8-hydroxyquinoline bridging ligands. This observation is in contrast with the calculated triplet spin density of previously published dinuclear Pt(II) complexes where MMLCT character is evident.[53] From analysis of the calculated orbitals of **1** and **2**, it becomes evident that the lowest energy transition is instead a mixed MLCT/LC transition, as the HOMO in both instances has both metal and hydroxyquinoline character while the LUMO is centred on the hydroxyquinoline bridges (Figs. S13 and S14). From these observations, it follows that **1** and **2** have diminished interaction between the Pt(II) centres compared to analogous dinuclear complexes, and likely behave as mononuclear species. This was confirmed by comparing the calculated properties of the mononuclear model complex, **3**, as shown in Fig. S15 and S18. Given that both the ground and excited state orbital contributions of **3** exactly

mirror what was observed from **1** and **2**, this confirms that the excited state characteristics of these new dinuclear complexes are more closely aligned with a mononuclear species than previously studied dinuclear systems.

Electronic Spectra

The electronic absorption spectra for **1-3** collected in THF are presented in Fig. 2 and summarized in Table 1. By comparing the observed electronic absorption spectra of the dinuclear complexes presented here to those of previous studies, it can be determined that the character of **1** and **2** more closely resembles mononuclear Pt(II) complexes such as the model system, **3**, than comparable dinuclear species. Analysis of the collected spectra in Fig. 1 indicates that the absorption features for **1-3** are very similar with near direct mapping of the broad peak of the lowest energy transition. The λ_{max} for this transition occurs at 484 nm and 475 nm for **1** and **2**, respectively, and 488 nm for species **3**. In previous studies of **3**, this transition was determined to be mixed in MLCT/LC character.[55,65] Given the comparable shape and molar extinction coefficient (ε), the lowest energy peak of **1** and **2** can also attributed to a LC/MLCT transition. DFT calculations (Figs. S13 and S14) confirm this assignment (*vide infra*). This differs with previous studies of Pt(II)-Pt(II) dinuclear species in which the lowest energy peak is assigned as an MMLCT transition and is significantly red-shifted compared to mononuclear systems due to interaction between the two metal centres. Specifically, in the case where the 8-hydroxyquinoline bridges are replaced by a substituted 2-hydroxypyridine (R = Me or Ph), this transition was observed between 500-600 nm – red shifted compared to an MLCT transition.[53] Instead, the observed lowest energy absorption of the dinuclear species of this study occurs at slightly bluer wavelengths than the mononuclear complex. Therefore, the results of the electronic absorption spectra of **1** and **2** align with the conclusions deduced from the calculations and further demonstrate that the dinuclear complexes here do not display any significant interactions between the Pt(II) centres, but instead behave as mononuclear species.
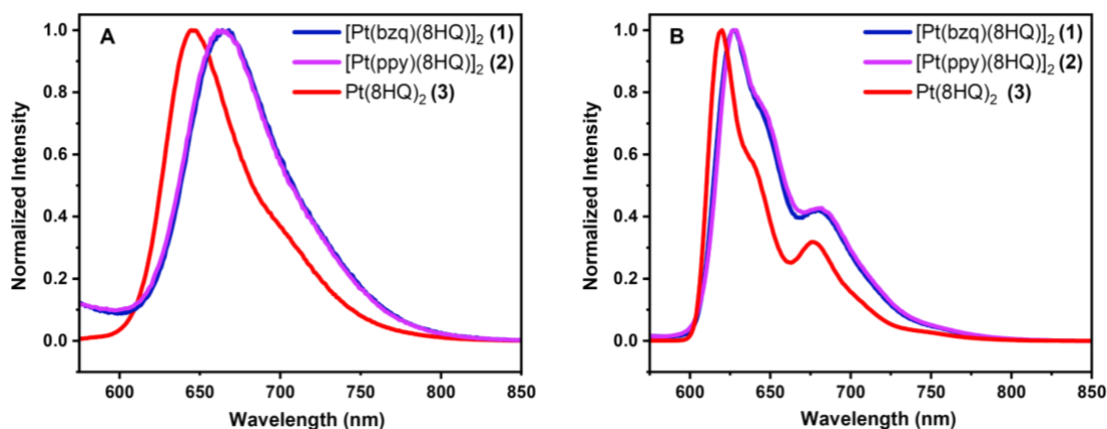

Fig. 3 Photoluminescence spectra of **1** - **3** resulting from 500 nm excitation measured at room temperature in THF (a) and 77K in 2-MeTHF (b).

Table 1. Spectroscopic and Photophysical Properties of **1** and **2** in THF (298K) and 2Me-THF (77K), using 500 nm excitation for emission and lifetime measurements.

	λ_{abs} (nm)	λ_{em}(nm, 298K)[a]	λ_{em} (nm, 77K)[b]	ϕ_{em}[c]	τ_{em} (µs)	k_r*10^{-4} (s^{-1})[d]	k_{nr}*10^{-6} (s^{-1})[e]
1	483, 376	679, 730	628, 651, 680	0.0082	4.2	0.195	0.236
2	476, 370	679, 730	628, 650, 682	0.0080	4.2	0.190	0.236

[a] in THF; [b] in 2-MeTHF; [c] ϕ_{em} is measured using Ru(bpy)$_3$(PF$_6$)$_2$ in CH$_3$CN as a quantum yield standard; [d]$k_r = \Phi_{PL}/\tau_{PL}$; [e]$k_{nr} = (1 - \Phi_{PL})/\tau_{PL}$

Photoluminescence

Room temperature photoluminescence of **1-3** was investigated in THF (Fig. 3a). The photoluminescence spectra of **1** and **2** are nearly identical, suggesting the same emitting state is being observed in both complexes. The maximum emission intensity occurs at 661 nm and 664 nm, respectively, each with a shoulder at 735 nm as summarized in Table 1. This differs in comparison to photoluminescence spectra of previously studied Pt(II)-Pt(II) complexes with the same bridge wherein modification of the cyclometalating ligand resulted in a shift of the observed [3]MMLCT emission. Specifically, dinuclear complexes having the C^N ligand 7,8-benzoquinoline generally demonstrate red-shifted emission features relative to those of 2-phenylpyridine due to the lower energy of the extended π-system.[53,54] These shifts range from 185 cm^{-1} – 370 cm^{-1}.[53,54] However, the emission peaks of **1** and **2** are separated by only 68 cm^{-1} despite having different cyclometalating ligands. This suggests that the emitting state of **1** and **2** does not have cyclometalating ligand character given that the observed spectra do not change with structural modification in the C^N ligands, leading to the conclusion that this emission cannot be from an [3]MMLCT state as in previously studied dinuclear species of similar structure. Additionally, the PL emission spectrum of **3** was collected in THF and found to have identical spectral shape as that of the dinuclear complexes with peaks slightly blue shifted to 645 nm and a corresponding shoulder at 715 nm. Given the similarity in PL spectral profile, it follows that the emission is likely emanating from the same state in all three molecules, **1-3**. In previous studies of **3** and similar complexes, this emission was determined to be from an excited state centred on 8-hydroxyquinoline.[65,66] This is supported by results from TD-DFT in which it was found that the electron densities of the lowest energy triplet state in all three chromophores is predominantly centred on the 8HQ ligand. This leads to the conclusion that the emission observed from **1-3** is from a [3]8HQ LC excited state.

Additionally, the photoluminescence spectra of **1** and **2** acquired at 77 K in 2-methyltetrahydrofuran (2-MeTHF) are also structured and have maxima at 628 nm and a shoulder at around 680 nm as shown in Fig. 3b. The structure observed from **3** is again identical with prominent features at 620 nm and 676 nm. While the similarity in the PL spectral shapes of **1** and **2** in comparison to the model system of **3** seems sufficient to suggest that the emitting states in all three complexes are the same hydroxyquinoline centred ligand state, the impact of temperature can provide further confirmation of these assignments. The thermally induced Stokes' shift observed between 77 K and 298 K was 795 cm^{-1} (**1**) and 863 cm^{-1} (**2**). This can be compared to a corresponding shift of 625 cm^{-1} present in **3**. This Stokes' shift results from the diminishing polarity of the solvent in the solid state at 77 K, decreasing stabilization of the excited state. As ligand-centred states are less affected by solvent stabilization with respect to charge transfer states, the modest blue shift of λ_{em} at 77 K compared to room temperature provides further evidence that the excited state cannot be charge transfer in nature but more closely aligns with a ligand centred excited state. These observations are consistent with the assignment of photoluminescence from a [3]8HQ LC state in **1**-**3**.

Nanosecond Transient Absorption Spectroscopy and Time Resolved Photoluminescence

Complexes **1-3** were analysed by nanosecond transient absorption (*ns*TA) spectroscopy to study their excited state dynamics. The transient absorption difference spectra of **1** (Fig. 4a) and **2** (Fig. S8) following a 500 nm laser pulse show similar excited state signatures and decay processes. Briefly, a ground state bleach is present at 480 nm in addition to two excited state features, with the first being centred at 400 nm and the second ranging from 500-800 nm. Single wavelength kinetics of the excited state features and ground state bleaches yield similar lifetimes of approximately 4 µs. This is considerably longer than the lifetimes of previously reported Pt(II) dinuclear complexes.[53] When compared to the *ns*TA difference spectrum of **3** in Fig. 4b, there is again remarkable similarity in spectral profile between the dinuclear and mononuclear species. The excited state absorption features of **3** are shifted slightly to 410 nm and 570-800 nm, as well as the ground state bleach at 500 nm. Kinetic decay studies at each of these single wavelength features indicates an excited state lifetime of approximately 5.1 µs, resembling the reported decay time constants for **1** and **2** (Fig. 4c). The similar spectral shape and comparable excited state lifetimes of **1-3** indicates that the excited state observed on the nanosecond timescale is likely the same for each of the three molecules. This excited state is therefore assigned to be the lowest energy [3]LC state of the 8HQ ligand. In support of this, the kinetic PL emission intensity decay of **1** at 680 nm is presented in Fig. 4d and Table 1, yielding a 4.2 µs lifetime, and aligns well with the lifetime ascertained using transient absorption kinetics. The same lifetime for the emitting
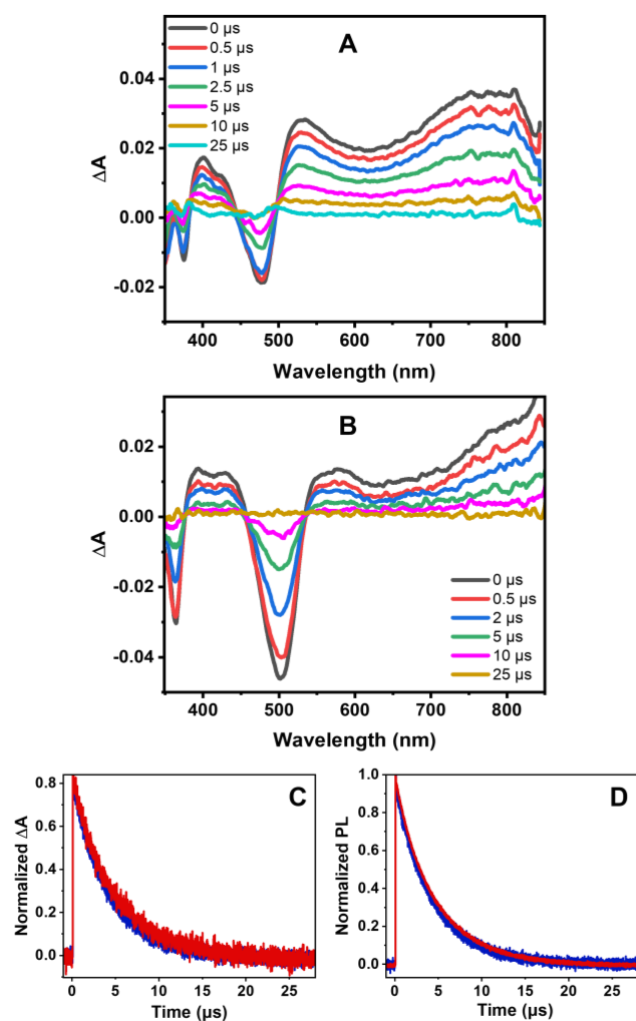
Fig. 4 Excited state absorption difference spectra of **1** (A) and **3** (B) (2 mJ/pulse, 7 nm fwhm). C) Kinetic absorption decay of **1** (red, λ_{detect} = 530 nm) and **3** (blue, λ_{detect} = 540 nm). Kinetic emission decay of **1** (680 nm) and **3** (650 nm) (All samples were examined in deaerated THF with 500 nm excitation)

nm, a broad absorption from 525-625 nm, and a near-infrared (NIR) feature centered at 1200 nm. This excited state is assigned to be [1]LC on the 8HQ ligand generated within the laser pulse duration. At later decay times, the shape of the difference spectra corresponds with that observed by *ns*TA, specifically with the growth of an excited state absorption feature at 700 nm. This suggests that the [1]LC state initially formed upon laser excitation undergoes direct intersystem crossing (ISC) to the lowest energy [3]LC state within 15 ps, which then persists into the nanosecond time regime and beyond as observed in *ns*TA experiments.

When the same *fs*TA experiment was performed on the model mononuclear complex **3** (Fig. S12), a similar spectral shape was observed as with **1** and **2** except for slightly different decay patterns in the redder wavelengths. For example, an excited state absorption feature grows in at 540 nm while another centered at 650 nm decays. However, there is still a growth of an excited state absorption feature centered at 400 nm and the same intense NIR feature was also observed which decays on the same time scale to form the persistent TA feature observed in *ns*TA. This suggests generation of [1]LC state on 8HQ followed by ISC to the [3]LC state as observed with **1** and **2**. However, for the model **3**, a ~200 nm red shift of λ_{max} of the NIR feature was observed with respect to the dinuclear species. This might be due to slight adjustment of the excited state energies of the cyclometalating ligands in the dinuclear complexes. Single-wavelength kinetic analysis of the *fs*TA difference spectra was performed at different wavelengths with the decays being fit to

state was observed in **2**, Fig. S9. Additionally, the kinetic emission of **3** measured at 650 nm yielded a lifetime of 5.3 μs in quantitative agreement with an excited state lifetime of 5.1 μs with consideration of experimental error. Given that the excited state and the emitting state have the same lifetimes, it follows that the excited state can be assigned as the lowest energy [3]LC state centred on the 8-hydroxyquinoline ligand as determined by the combined experimental and computational data.

Femtosecond Absorption Spectroscopy (*fs*TA)

Femtosecond (*fs*) laser pump-probe experiments were performed to observe early timescale excited state features for the molecules in this study. Differential femtosecond transient absorption (*fs*TA) spectra following 500 nm excitation in THF for **1** and **2** are presented in Fig. 5. The excited state difference spectra of both molecules evolve with similar spectral signatures and time constants. The initially populated excited state possesses a sharp feature near 400
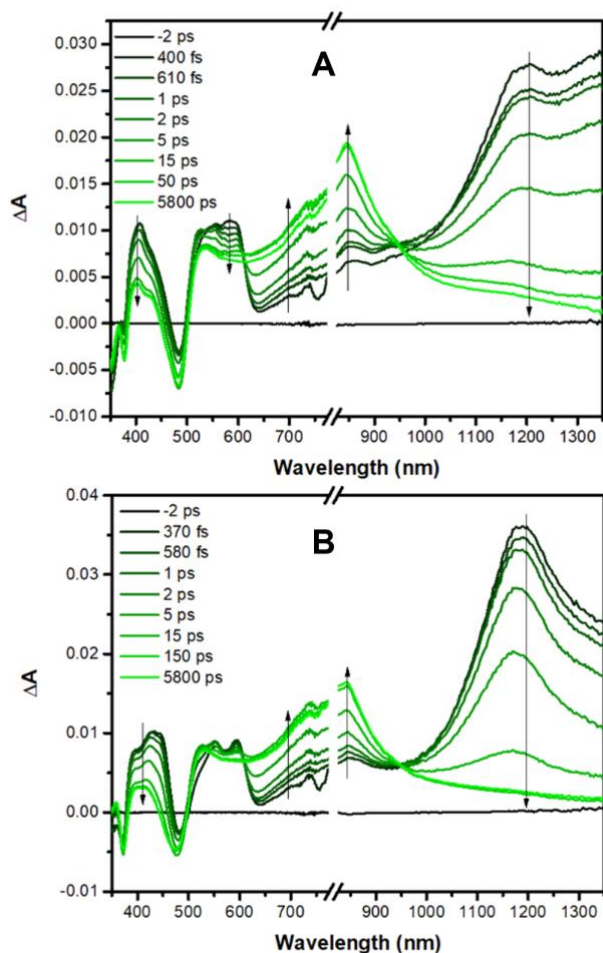
Fig. 5 Femtosecond transient absorbance difference spectra of (A) **1** and (B) **2** after photoexcitation at 500 nm in THF

multiexponential parameters (Figs. S10 and S11). The time constants obtained from these kinetic analyses were similar for both molecules. The shortest time constants (τ_1 = 5-8 ps) were assigned to ISC from the [1]LC to [3]LC state on 8HQ. This is followed by a longer time constant (τ_2 = 25-45 ps) likely arising due to conformational changes in the dinuclear complexes. Finally, the [3]LC excited state decays back to ground state with a long lifetime (τ_3 = 3.5-3.8 µs).

Conclusions

Presented here are the synthesis and characterization of two newly conceived platinum(II) dinuclear complexes bridged by two 8-hydroxyquinolines, coordinated by cyclometalating 7,8-benzoquinoline (**1**) or 2-phenylpyridine (**2**) ligands. When compared to previously studied Pt(II)-Pt(II) complexes as well as the mononuclear model system **3**, it becomes apparently clear that the photophysical behaviour of **1** and **2** is more closely aligned with mononuclear complexes than with traditional Pt(II) dinuclear species featuring MMLCT excited states. As first observed in the calculated electronic excited state properties, there was little

evidence for interactions between the two metal centres. This was then observed experimentally in the electronic absorption spectra of **1** and **2** wherein the lowest energy transitions were assigned to be of mixed LC/MLCT character resembling that of model, **3**. Additionally, the lowest energy triplet state of **1** and **2** was determined to be ligand-centred and focused on the 8-hydroxyquinoline bridge by photoluminescence and transient absorption spectroscopy, contrasting with previous Pt(II)-Pt(II) dinuclear chromophores wherein the emitting state was of [3]MMLCT character. As a result, remarkable similarity was noted in the photoluminescence spectra of all three complexes at both room temperature and 77 K. Further, time resolved spectroscopic experiments indicated that that the excited states of **1** and **2** are comparatively long-lived. Excitation at 500 nm initially produces the 8HQ [1]LC state which undergoes intersystem crossing to produce the [3]LC state within 15 ps as observed in *fs*TA experiments. This excited state then persists for approximately 4 µs, determined by *ns*TA. This is comparable to the excited state lifetime of 5.1 µs observed in **3**. Finally, the observed absorption difference spectra of **1**-**3** all exhibited similar spectral shape and decay/recovery patterns in both nsTA and *fs*TA, further confirming that the dinuclear complexes in this study behave like mononuclear chromophores, whose metal-metal distances are simply too remote to enable any σ-interactions whatsoever.

Author Contributions

[†] These authors contributed equally. The manuscript was written through the contributions of all authors. All authors have given approval to the final version of the manuscript.

Conflicts of interest

"There are no conflicts to declare".

Acknowledgements

References

(1) H. Xu, R. Chen, Q. Sun., W. Lai, ., Q. Su,W. Huangand X. Liu, *Chem. Soc. Rev.,* 2014, **43**, 3259-3302.

(2) K. Kalyanasundaram,*Coord. Chem. Rev.,* 1998, **177**, 347-414.

(3) K. Li, G. S. Ming Tong, Q. Wan, G. Cheng, W. Y. Tong,W. H. Ang, W. L. Kwong and C. M. Che, *Chem. Sci.,* 2016, **7**, 1653-1673.

(4) H. Yersin, A. F. Rausch, R. Czerwieniec, T. Hofbeck and T. Fischer, *Coord. Chem. Rev.,* 2011, **255**, 2622-2652.

(5) M. Hissler, J. E. McGarrah, W. B. Connick, D. K. Geiger, S. D. Cummings and R. Eisenberg, *Coord. Chem. Rev.,* 2000, **208**, 115-137.

(6) W. B. Connick and H. B. Gray, *J. Am. Chem. Soc.,* 1997, **119**, 11620-11627.

(7) R. C. Evans, P. Douglas and C. J. Winscom, *Coord. Chem. Rev.,* 2006, **250**, 2093-2126.

(8) J. A. Bailey, M. G. Hill, R. E. Marsh, V. M. Miskowski, W. P Schaefer and H. B. Gray, *Inorg. Chem.,* 1995, **34**, 4591-4599.

(9) W. B. Connick, R. E. Marsh, W. P. Schaefer and H. B. Gray, *Inorg. Chem.,* 1997, **36**, 913-922.

(10) S. W. Lai, H. W. Lam, W. Lu, K. K. Cheung and C. M. Che, *Organometallics,* 2002, **21**, 226-234.

(11) V. M. Miskowski and V. H. Houlding, *Inorg. Chem.,* 1989, **28**, 1529-1533.

(12) V. M. Miskowski and V. H. Houlding, *Inorg. Chem.,* 1991, **30**, 4446-4452.

(13) V. W. W. Yam, K. M. C. Wongand N. Zhu, *J. Am. Chem. Soc.,* 2002, **124**, 6506-6507.

(14) H. Yersin, D. Donges, W. Humbs, J. Strasser, R. Sitters and M. Glasbeek, *Inorg. Chem.* 2002, **41**, 4915-4922.

(15) W. Lu, B. X. Mi, M. C. W. Chan, Z. Hui, C. M. Che, N. Zhu and S.T. Lee, *J. Am. Chem. Soc,* 2004, **126**, 4958-4971.

(16) B. Ma, P. I. Djurovich, M. Yousufuddin, R. Bau and M. E. Thompson, *J. Phys. Chem. C,* 2008, **112**, 8022-8031.

(17) J. E. McGarrah, Y. J. Kim, M. Hisslerand R. Eisenberg, *Inorg. Chem.,* 2001, **40**, 4510-4511.

(18) W. Y. Wong, Z. He, S. K. So, K. L. Tongand Z. Lin, *Organometallics,* 2005, **24**, 4079-4082.

(19) D. Zhang, L. Z. Wu, L. Zhou, X. Han, Q. Z. Yang, L. P. Zhang and C. H. Tung, *J. Am. Chem. Soc.J. Am. Chem. Soc,* 2004, **126,** 3440-3441.

(20) K. H. Wong, M. C. W. Chan and C. M. Che, *Chem. Eur. J.,* 1999, **5**, 2845-2849.

(21) P. H. Lanoë, J. L. Fillaut, L. Toupet, J. A. G. Williams, H. L. Bozec and V. Guerchais, *Chem. Comm.,* 2008, 4333.

(22) X. Wang, S. B. Goeb, Z. Ji, N. A. Pogulaichenkoand F. N. Castellano, *Inorg. Chem.,* 2011, **50**, 705-707.

(23) B. Ma, P. I. Djurovich, S. Garon, B. Alleyneand M. E. Thompson, *Adv. Funct. Mat.,* 2006, **16**, 2438-2446.

(24) A. A. Rachford, and F. N. Castellano, *Inorg. Chem.,* 2009, **48**, 10865-10867.

(25) F. N. Castellano, *Dalton Trans.,* 2012, **41**, 8493-8501.

(26) F. N. Castellano, Felix N., *Acc. Chem. Res.* 2015, **48**(3), 828-839.

(27) Y. E. Begantsova, L. N. Bochkarev, S. Y. Ketkov, E. V. Baranov, M. N. Bochkarevand D. G. Yakhvarov, *J. Organomet. Chem.,* 2013, **733**, 1-8.

(28) C. L. Ho, W. Y. Wong, G. J. Zhou, B. Yao, Z. Xieand L. Wang, *Adv. Funct. Mater.,* 2007, **17**, 2925-2936.

(29) V. Sicilia, P. Borja and A. Martín, *Inorganics,* 2014, **2**, 508-523.

(30) Y. Xu, Y. Luo, M. Li, R. Heand W. Shen, *J. Phys. Chem. A,* 2016, **120**, 6813-6821.

(31) Y. Yasunori, M. Reina, K. Daishin and K. Masayuki, *Inorg. Chim. Acta,* 2021, **515**, 120049.

(32) M. Chaaban, C. Zhou, H. Lin, B. Chyiand B. Ma, *J. Mater. Chem.C,* 2019, **7**, 5910-5924.

(33) J. V. Lockard, A. A. Rachford, G. Smolentsev, A. Strickrath, X. Wang, X. Zhang, K. Atenkoffer, G. Jennings, A. Soldatov, A. L. Rheingold, F. N. Castellano and L. X. Chen, *J. Phys. Chem. A,* 2010, **114**, 12780-12787

(34) S. Cho, M. W. Mara, X. Wang, J. V. Lockard, A. A. Rachford, F. N. Castellanoand L. X. Chen, *J. Phys. Chem. A,* 2011, **115**, 3990-3996.

(35) S. Brown-Xu, M. Kelley, K. Fransted, A. Chakraborty, G. Schatz, F. N. Castellanoand *L. X.* Chen, *J. Phys. Chem. A,* 2016, **120**, 543-550.

(36) K. Haldrup, A. Dohn, M. L. Shelby, M. W. Mara, A. B. Stickrath, M. R. Harpham, J. Huang, X. Zhang, K. B. Møller, A. Chakraborty, F. N. Castellano, D. M. Tiede and L. X. Chen, *J. Phys. Chem. A,* 2016, **120**, 7475-7483.

(37) D. B. Lingerfelt, P. J. Lestrange, J. Radler, S. E. Brown-Xu, P. Kim, F. N. Castellano, L. X. Chen and X. Li, *J. Phys. Chem. A,* 2017, **121**, 1932-1939.

(38) P. Kim, M. S. Kelley, A. Chakraborty, N. L. Wong, R. P. Van Duyne, G. C. Schatz, F. N. Castellanoand L. X. Chen, *J. Phys. Chem. J. Phys. Chem. C,* 2018, **122**, 14195-14204.

(39) J. J. Radler, D. B. Lingerfelt, F. N. Castellano, L. X. Chen and X. Li, *J. Phys. Chem. A,* 2018, **122**, 5071-5077.

(40) A. J. S. Valentine, J. J. Radler, F. N. Castellano, L. X. Chenand X. Li, *J. Chem. Phys.,* 2019, **151**, 114303.

(41) P. Kim, A. J. S. Valentine, S. Roy, A. W. Mills, A. Chakraborty, F. N. Castellano, X. Liand L. X. Chen, *J. Phys. Chem. Lett.,* 2021, **12**, 6794-6803.

(42) A. Mills, A. Valentine, K. Hoang, S. Roy, F. N. Castellano, L. X. Chen, X. Li, *J. Phys. Chem. A,* 2021, **125**, 9438-9449.

(43) P. Kim, A. J. S. Valentine, S. Roy, A. W. Mills, F. N. Castellano, X. Liand L. X. Chen, *Faraday Discuss.,* 2022, **237**, 259-273.

(44) T. W. Kim, P. Kim, A. W. Mills, A. Chakraborty, S. Kromer, A. J. S. Valentine, F. N. Castellano, X. Li and L. X. Chen,. *J. Phys. Chem. C,* 2022, **126**, 11487–11497.

(45) S. Akatsu, Y. Kanematsu, T. A. Kurihara, S. Sueyoshi, Y. Arikawa, M. Onishi, S. Ishizaka, N. Kitamura, Y. Nakao, S. Sakaki and K. Umakoshi, *Inorg. Chem.,* 2012, **51**, 7977-7992.

(46) A. Chakraborty, J. C. Deaton, A. Haefele and F. N. Castellano, *Organometallics,* 2013, **32**, 3819-3829.

(47) M. Han, Y. Tian, Z. Yuan, L. Zhu and B. A. Ma, *Angew. Chem. Int. Ed.,* 2014, **53**, 10908-10912.

(48) S. W. Lai, M. C. W. Chan, T. C. Cheung, S. M. Peng and C. M. Che, *Inorg. Chem.,* 1999, **38**, 4046-4055.

(49) S. W. Lai, M. C. W. Chan, K. K. Cheung, S. M. Peng amd C. M. Che, *Organometallics,* 1999, **18**, 3991-3997.

(50) B. Ma, J. Li, P. I. Djurovich, M. Yousufuddin, R. Bau and M. E. Thompson, *J. Am. Chem. Soc.,* 2005, **127**, 28-29.

(51) C. E. McCusker, A. Chakraborty and F. N, Castellano, *J. Phys. Chem. A,* 2014, **118**, 10391-10399.

(52) C. Zhou, L. Yuan, Z. Yuan, N. K. Doyle, T. Dilbeck, D. Bahadur, S. Ramakrishnan, A. Dearden,C. HuangB. Ma, *Inorg. Chem.,* 2016, **55**, 8564-8569.

(53) A. Chakraborty, J. E. Yarnell, R. D. Sommer, S. Roy and F. N. Castellano, *Inorg. Chem.* **2018**, *57*, 1298-1310.

(54) S. Roy, A. A. Lopez, J. E. Yarnell and F. N. Castellano, *Inorg. Chem.,* 2022, **61**, 121-130.

(55)   R. Ballardini, G. Varani, M. T. Indelliand F. Scandola, *Inorg. Chem.,* 1986, **25**, 3858-3865.

(56)   J. Brooks, Y. Babayan, S. Lamansky, P. I. Djurovich, I. Tsyba, R. Bauand M. E. Thompson, *Inorg. Chem.,* 2002, **41**, 3055-3066.

(57)   V. Y. Kukushkin, A. J. L. Pombeiro, C. M. P. Ferreira and L. I. Elding, *Inorganic Syntheses* 2002, **33**, 189-196.

(58)   M. J. Frisch, G. W. Trucks, H. B. Schlegel, G. E. Scuseria, M. A. Robb, J. R. Cheeseman, G. Scalmani, V. Barone, G. A. Petersson, H. Nakatsuji, X. Li, M. Caricato, A. Marenich, J. Bloino and B. G. Janesko, *Gaussian 09, Revision D.01*; Gaussian, Inc.: Wallingford, CT, 2009.

(59)   C. Adamo and V. Barone, *J. Chem. Phys.,* 1999, **110**, 6158-6170.

(60)   F. Weigendand R. Ahlrichs, *Phys. Chem. Chem. Phys.,* 2005, **7**, 3297.

(61)   D. Andrae, U. Häußermann, M. Dolg, H. Stoll and H. Preuß, *Theoretica Chimica Acta* 1990, **77**, 123-141.

(62)   M. Cossi, G. Scalmani, N. Rega, V. Barone, *J. Chem. Phys.* 2002, **117**, 43-54.

(63)   S. Grimme, J. Antony, S. Ehrlichand H. Krieg, *J. Chem. Phys.,* 2010, **132**, 154104.

(64)   K. Tamami, A. Omura, and M. Kato, *Chem. Lett.,* 2004, **33**, 1386-1387.

(65)   D. Donges, J. K. Nagle and H. Yersin, *Inorg. Chem.*, 1997, **36**, 3040-3048.

(66)   N. M. Shavaleev, H. Adams, J. Best, R. Edge, S. Navaratnam and J. A. Weinstein, *Inorg. Chem.*, 2006, **45**, 9410-9415.